Transactions of the Nigerian Association of Mathematical Physics
Volume 11, (January - June, 2020 Issue), pp161 – 172

EFFECTS OF VARIABILITY IN VISCOSITY AND THERMAL CONDUCTIVITY ON STEADY MIXED CONVECTION COUETTE FLOW AND HEAT TRANSFER

Abiodun O. Ajibade[1] and Tafida M. Kabir[2]

[1]Department of Mathematics, Ahmadu Bello University, Zaria, Nigeria.
[2]Department of Mathematics, Federal College of Education, Zaria, Nigeria

Abstract

An investigation on effects of variability in viscosity and thermal conductivity on steady mixed convection flow and heat transfer in a vertical channel is carried out. The equations of momentum and energy were solved analytically using Homotopy perturbation method. The impacts of the several controlling parameters were investigated and discussed. From the course of investigation, it was found that fluid velocity and temperature increase at fluid section near the heated plate while it decrease at section near the cold plate as the viscosity increases. The thermal conductivity decreases the fluid velocity gets increased at the heated plate while the reverse case was observed at the cold plate. It was further found that a higher mixed convection parameter leads to induce a reverse flow.

Keywords: thermal conductivity; variable viscosity; mixed convection; Couette flow; Homotopy perturbation method.

Nomenclature

g -acceleration due to gravity [ms^{-2}]
β -coefficient of thermal expansion $[K^{-1}]$
T^* - dimensional fluid temperature $[K]$
T_w - channel wall temperature $[K]$
T_0 - temperature of the ambience $[K]$
T - dimensionless fluid temperature
U - dimensional velocity of the moving plate[ms^{-1}]
y - dimensionless co-ordinate perpendicular to the plate
y^*-co-ordinate perpendicular to the plate [m]
α - thermal diffusivity of the fluid $[Kgm^{-3}]$
c_p - specific heat at constant pressure $[m^2s^{-2}K^{-1}]$
S -dimensionless heat generation/absorption parameter
μ -coefficient of viscosity $[Kgm^{-1}s^{-1}]$
Q_0 -heat generation/absorption coefficient $[Kgm^{-1}s^{-3}K^{-1}]$
Pr - Prandtl number
Gr - Grashof number
Re - Reynold number
Ec - Eckert number
ρ - density of the fluid $[Kgm^{-3}]$
u^* - dimensional velocity [ms^{-1}]
h-width of the channel [m]
u^* - dimensional velocity [ms^{-1}]
p -embedding parameter
υ - kinematic viscosity [m^{2}s^{-1}]

1 Introduction

The study of mixed convection flow between vertical channels has considerable applications in Geophysics and many Engineering problems, such as cooling nuclear reactors safety analysis, metal waste, spent nuclear fuel and fire. An unsteady mixed convection flow past an infinite vertical porous with constant heat source has been considered by Jha [1]. He concluded that fluid velocity decreases with the increase of heat source. Jha and Ajibade [2] also carried out extensive study of an unsteady free convective Couette flow of heat generating/absorbing fluid. They discovered that increasing the internal heat absorption decreases the skin friction on both plates, while the mass flux is shown to be higher for mercury as compared to air since mercury possesses higher temperature and velocity than air. Jer-Huan et al. [3] investigated wall transpiration effects on mixed convection and concluded that rate of heat transfer increases with an increase in mixed convection parameter. Jha et al. [4] presented steady fully developed mixed convection flow in a vertical parallel micro channel with porous material. They found that increasing values of mixed convection parameter leads to decrease in fluid velocity. Hamid and Behnam [5] considered mixed convective rarefied flows with symmetric and asymmetric heated walls. They discovered that the friction coefficient increases and decreases with growing mixed convection parameter on the hot and cold walls. Borah and Hazarika [6] studied the effects of variable viscosity and thermal conductivity effect on the free convection and mass transfer flow. They showed that the temperature decreases with the increase of both viscosity and thermal

Correspondence Author: Tafida M.K., Email: mktafida.555@gmail.com, Tel: +2348065539821

conductivity parameter. Hazeem and Mostafa [7] presented a study on the efficiency of variation of physical variables on steady flow between parallel plates with heat transfer. It was discovered that the viscosity and the thermal conductivity parameter have a more evident effect on the velocity and temperature distributions for smaller values of porosity parameter. On the other hand, the thermal conductivity has no substantial effect on the velocity. However, it has a marked effect on the temperature. Mohamed [8] analyzed unsteady mixed convection heat transfer along vertical stretching surface with variable viscosity. They reported that growing values of mixed convection parameter is to enhance the local heat transfer rate for all values of viscosity. Swati and Iswar [9] studied magnetohydrodynamics mixed convection and heat transfer over a vertical porous plate. They concluded that fluid velocity increases with the increase in mixed convection. Parash and Hazarika [10] investigated effects of variable viscosity and thermal conductivity on unsteady free convective heat and mass transfer. They discovered that viscosity and thermal conductivity have significant effects on velocity and temperature distributions within the boundary layer. Anjali-Devi and Prakash [11] studied the temperature dependent viscosity and thermal conductivity effects on hydromagnetic flow. Their work discovered that the temperature increases with the increase in thermal conductivity. Makungu et al. [12] examined the effect of variable viscosity and thermal radiation over a permeable wedge embedded in saturated porous medium with chemical reaction. They reported that the heat transfer rate increase with the increase in viscosity. Santana and Hazarika [13] investigated the effects of variable viscosity and thermal conductivity on magnetohydrodynamics free convection and mass transfer flow over an inclined vertical surface with heat generation. They discovered that an increase of thermal conductivity fluid temperature decreases. Macha and Naikoti [14] presented mixed convection analysis of heat and mass transfer. They showed that fluid velocity increases with an increase in mixed convection parameter whereas increasing values of mixed convection parameter decreases the temperature profile. Muhammad et al. [15] studied viscous dissipation effect on the mixed convection boundary layer flow. They found that an increase in mixed convection parameter and Prandtl number has decreased the thermal boundary layer thickness. Prathap et al. [16] presented viscous dissipation on mixed convection flow using Robin boundary conditions. They discovered that an increasing mixed convection parameter increases the reversal of flow at both plates. Hazarika and Bandita [17] analyzed the effects of variable viscosity and thermal conductivity on magnetohydrodynamics free convection flow of a micropolar fluid past a stretching plate through porous medium with radiation, heat generation and joule dissipation. They showed that thermal conductivity decreasing the temperature whereas viscosity increases it. Ajibade and Thomas [18] studied entropy generation due to steady mixed convection flow in a vertical porous channel. They reported that fluid velocity increases with an increase in mixed convection parameter. Jha and Aina [19] analyzed effect of induced magnetic field on magnetohydrodynamics mixed convection flow in a vertical micro-channel. They reported that increasing the mixed convection parameter leads to a reduction in the fluid velocity at the cold wall while the reverse trend is observed at the heated wall. Ajibade and Tafida [20] examined viscous dissipation effect on steady natural convection Couette flow of heat generating fluid in a vertical channel. They discovered that fluid temperature and velocity increase with an increase in viscous dissipation. In another article, Ajibade and Tafida [21] considered viscous dissipation effect on a steady generalised Couette flow of heat generating/absorbing fluid in a vertical. They reported that fluid temperature and velocity increase with an increase in Eckert number.

The objective of the present study is to investigate the effects of variability in viscosity and thermal conductivity on steady mixed convection flow and heat transfer in a vertical channel. The equations governing the flow are non linear and coupled so that obtaining closed form solution is a daunting task. Such problems can therefore be approached by numerical schemes or some approximate solution methods. One of the efficient methods is the perturbation method. However, solutions obtained by perturbation method are restricted to small perturbation parameters; therefore to overwhelm this restriction, alternative method called Homotopy perturbation method was presented. The convergence of the Homotopy perturbation method is so rapid that just a few terms of the series solution is required to achieve a high accuracy of the solutions.

The concept of Homotopy Perturbation Method (HPM) was initially introduced by He [22] to solve linear, non-linear and coupled equations in partial or ordinary form. He [23] studied a coupling method of a Homotopy technique and perturbation technique for non-linear problems. He [24] studied a new non-linear analytical technique using Homotopy perturbation method. He [25] also introduce the new method to solve non-linear and boundary value problems (BVP) and further established the Homotopy perturbation method for solving nonlinear initial and boundary value problems by combining the standard Homotopy in topology and the perturbation technique. By this method, a speedy convergent series solution can be obtained in most of the cases. Normally, a few terms of the series solution can be used for numerical calculations. Abaker [26] analyzed solution of linear and non linear Schrodinger equation using Homotopy perturbation method and variational iteration method. They concluded that Homotopy perturbation method is very efficient and powerful to get the exact solution and also gives more sensible series solutions that converge very fast in physical problems. Because of nonlinearity and coupling of the governing equations in the present situation, the Homotopy perturbation shall be engaged to obtain the solutions. Abou-Zeid [27] examined Homotopy perturbation method for magnetohydrodynamics non-Newtonian nanofluid flow through a porous medium in eccentric annuli with peristalsis.

2 Mathematical Analysis

The present problem considers unsteady mixed convection flow of an incompressible viscous fluid in a vertical channel formed by two infinite parallel plates. The x^*- axis is taken vertically parallel to one of the plates of the channel and normal to the y^* - axis. The plate at $y=0$ moves impulsively in its own plane with uniform velocity U while the other plate, which is placed h distance away from the first one remain stationary. The fluid flow is set up due to the applied pressure gradient, movement of one of the channel plates as well as density change caused by the asymmetric heating of the channel boundary plates, hence, the present situation describes a mixed convection flow in a vertical channel. The flow configuration and coordinates system is shown in figure 1.

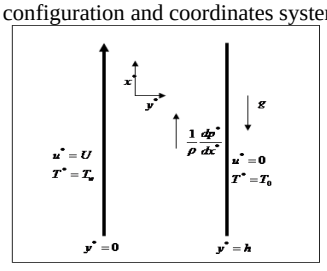

Figure 1: Schematic diagram of the problem

Under the usual assumption of Boussinesq's approximation, the governing dimensional equations of the energy and momentum are:

$$\frac{1}{\rho}\frac{d}{dy^*}\left(\mu^*\frac{du^*}{dy^*}\right)+g\beta(T^*-T_0)-\frac{1}{\rho}\frac{dP^*}{dx^*}=0. \quad (1)$$

$$\frac{1}{\rho c_p}\frac{d}{dy^*}\left(k^*\frac{dT^*}{dy^*}\right)-\frac{Q_0}{\rho c_p}(T^*-T_0)+\frac{\mu^*}{\rho c_p}\left(\frac{du^*}{dy^*}\right)^2=0, \quad (2)$$

Here u^* is the dimensional velocity, T^* is the dimensional temperature. y^* is the dimensional distance. β is the coefficient of thermal expansion, ρ is the density of the fluid, c_p is the specific heat constant pressure, Q_0 is the heat generation/absorption coefficient, k^* is the thermal conductivity, $\frac{dP^*}{dx^*}$ is the applied pressure gradient and g is the acceleration due to gravity.

The viscosity and thermal conductivity of the working fluid are assumed to vary linearly with temperature as follows

$$\mu^*=\mu_0(1-a(T^*-T_0)), \qquad k^*=k_0(1-b(T^*-T_0))$$

while the boundary conditions that satisfy the problem are:

$$u^*=U, T^*=T_w \text{ at } y^*=0,$$

$$u^*=0, T^*=T_0 \text{ at } y^*=h. \quad (3)$$

where U is the velocity of the moving plate, T_w is the temperature of the heated plate and T_0 temperature of the cold plate respectively. By introducing the following dimensionless quantities:

$$y=\frac{y^*}{h}, u=\frac{u^*}{U}, T=\frac{T^*-T_0}{T_w-T_0}, Ec=\frac{U^2}{c_p(T_w-T_0)}, \Pr=\frac{\mu c_p}{k}, Gr=\frac{g\beta h^3(\theta_w-\theta_0)}{\upsilon U}$$

$$S=\frac{Q_0h^2}{k}, P=\frac{P^*}{\rho U^2}, \lambda=a(T_w-T_0), x^*=\frac{x^*\nu}{Uh^2}, \mathrm{Re}=\frac{Uh}{\nu} \quad (4)$$

Where u is the dimensionless velocity, T is the dimensionless temperature, y is the dimensionless coordinate normal to the channel walls, Pr is the Prandtl number, S is the heat generation/absorption, μ the viscosity coefficient, Ec is the viscous dissipation and Gre is the ratio of Grashof number to that of the Reynolds number.

Applying the usual Boussinesq approximation to equations (1) and (2), the momentum and energy equations in the dimensionless form are

$$(1-\lambda T)\frac{d^2u}{dy^2}-\lambda\frac{du}{dy}.\frac{dT}{dy}+GreT-\frac{dP}{dx}=0, \quad (5)$$

$$(1-\varepsilon T)\frac{d^2T}{dy^2}-\varepsilon\left(\frac{dT}{dy}\right)^2-S(1-\varepsilon T)T+Ec\,\Pr(1-\varepsilon T)\left(\frac{du}{dy}\right)^2=0. \quad (6)$$

The boundary conditions in the dimensionless form for the physical system considered in the present work are:

$$u=1, T=1, \text{ at } y=0,$$

$$u=0, T=0, \text{ at } y=1. \quad (7)$$

2.1 Solution by Homotopy Perturbation Method

Apply the Homotopy perturbation technique to solve the governing equations in the present problem, we Construct a convex Homotopy on equations (5) and (6) to get

$$H(u,p)=(1-p)\left(\frac{d^2u}{dy^2}\right)+p\left(\frac{d^2u}{dy^2}-\lambda\frac{du}{dy}.\frac{dT}{dy}+GreT-\frac{dP}{dx}\right)=0, \quad (8)$$

$$H(T,p)=(1-p)\left(\frac{d^2T}{dy^2}\right)$$

$$+p\left(\frac{d^2T}{dy^2}-\varepsilon T\frac{d^2T}{dy^2}-\varepsilon\left(\frac{dT}{dy}\right)^2+Ec\,\Pr\left(\frac{du}{dy}\right)^2-\varepsilon Ec\,\Pr T\left(\frac{du}{dy}\right)^2-ST+\varepsilon ST^2\right)=0, \quad (9)$$

Simplify

$$\frac{d^2u}{dy^2}+p\left(GreT-\lambda\frac{du}{dy}.\frac{dT}{dy}-\frac{dP}{dx}\right)=0, \quad , \quad (10)$$

$$\frac{d^2T}{dy^2}+p\left(Ec\,\Pr\left(\frac{du}{dy}\right)^2-\varepsilon T\frac{d^2T}{dy^2}-\varepsilon\left(\frac{dT}{dy}\right)^2-\varepsilon Ec\,\Pr T\left(\frac{du}{dy}\right)^2-ST+\varepsilon ST^2\right)=0 \quad (11)$$

using infinite series (5) and (6) to define u and T as follows

$$u=u_0+pu_1+p^2u_2+\ldots,$$

$$T=T_0+pT_1+p^2T_2+\ldots, \quad (12)$$

Substituting (12) into (10) and (11) and simplifying, we have the following

$$\frac{d^2u_0}{dy^2}+p\frac{d^2u_1}{dy^2}+p^2\frac{d^2u_2}{dy^2}+....=p\frac{dP}{dx}-pGreT_0-p^2GreT_1-...$$
$$+p\lambda T_0\frac{d^2u_0}{dy^2}+p^2\left(\lambda T_0\frac{d^2u_1}{dy^2}+\lambda T_1\frac{d^2u_0}{dy^2}\right)+... \quad (13)$$
$$+p\lambda\frac{du_0}{dy}.\frac{dT_0}{dy}+p^2\left(\lambda\frac{du_0}{dy}.\frac{dT_1}{dy}+\lambda\frac{du_1}{dy}.\frac{dT_0}{dy}\right)+...$$

Similarly,

$$\frac{d^2T_0}{dy^2}+p\frac{d^2T_1}{dy^2}+p^2\frac{d^2T_2}{dy^2}+....=p\varepsilon T_0\frac{d^2T_0}{dy^2}+p^2\left(\varepsilon T_0\frac{d^2T_1}{dy^2}+\varepsilon T_1\frac{d^2T}{dy^2}\right)+...$$
$$+p\varepsilon\left(\frac{dT_0}{dy}\right)^2+p^2\left(2\varepsilon\frac{dT_0}{dy}.\frac{dT_1}{dy}\right)+...$$
$$-pEc\,\mathrm{Pr}\left(\frac{du_0}{dy}\right)^2-p^2\left(2Ec\,\mathrm{Pr}\frac{du_0}{dy}.\frac{du_1}{dy}\right)-... \quad (14)$$
$$+p\varepsilon Ec\,\mathrm{Pr}T_0\left(\frac{du_0}{dy}\right)^2$$
$$+p^2\left(2\varepsilon Ec\,\mathrm{Pr}T_0\frac{du_0}{dy}.\frac{du_1}{dy}+\varepsilon Ec\,\mathrm{Pr}T_1\left(\frac{du_0}{dy}\right)^2\right)+...$$
$$+pST_0+p^2ST_1+...$$
$$-p\varepsilon ST_0^2-p(2\varepsilon ST_0T_1)-...$$

By comparing the coefficient p^0, p^1 and p^2 of equation (13) and (14), we have

$$p^0:\frac{d^2u_0}{dy^2}=0, \quad (15)$$

$$p^0:\frac{d^2T_0}{dy^2}=0, \quad (16)$$

$$p^1:\frac{d^2u_1}{dy^2}=\frac{dP}{dx}-GreT_0+\lambda\frac{du_0}{dy}.\frac{dT_0}{dy}+\lambda T_0\frac{d^2u_0}{dy^2}, \quad (17)$$

$$p^1:\frac{d^2T_1}{dy^2}=\varepsilon T_0\frac{d^2T_0}{dy^2}+\varepsilon\left(\frac{dT_0}{dy}\right)^2-Ec\,\mathrm{Pr}\left(\frac{du_0}{dy}\right)^2-\varepsilon ST_0^2+\varepsilon Ec\,\mathrm{Pr}T_0\left(\frac{du_0}{dy}\right)^2+ST_0, \quad (18)$$

$$p^2:\frac{d^2u_2}{dy^2}=-GreT_1+\lambda\frac{du_0}{dy}.\frac{dT_1}{dy}+\lambda\frac{du_1}{dy}.\frac{dT_0}{dy}+\lambda T_0\frac{d^2u_1}{dy^2}+\lambda T_1\frac{d^2u_0}{dy^2}, \quad (19)$$

$$p^2:\frac{d^2T_2}{dy^2}=\varepsilon T_0\frac{d^2T_1}{dy^2}+\varepsilon T_1\frac{d^2T_0}{dy^2}+2\varepsilon\frac{dT_0}{dy}.\frac{dT_1}{dy}-2Ec\,\mathrm{Pr}\frac{du_0}{dy}.\frac{du_1}{dy}$$
$$+\varepsilon Ec\,\mathrm{Pr}T_1\left(\frac{du_0}{dy}\right)^2+ST_1+2\varepsilon Ec\,\mathrm{Pr}T_0\frac{du_0}{dy}.\frac{du_1}{dy}-2\varepsilon ST_0T_1, \quad (20)$$

.
.
.

The boundary conditions (7) are transformed also as

$$u_0(0)=1,u_1(0)=u_2(0)=u_3(0)...=0,$$
$$u_0(1)=u_1(1)=u_2(1)=u_3(1)...=0,$$
$$T_0(0)=1,T_1(0)=T_2(0)=T_3(0)...=0, \quad (21)$$
$$T_0(1)=T_1(1)=T_2(1)=T_3(1)...=0.$$

Since the zeroth order of the homotopy gives a linear ordinary differential equation, it is easily solvable without making recourse to initial guess. Therefore solving (15) and (16) and applying the boundary conditions $u_0(0)=1$ and $u_0(1)=0$, $T_0(0)=1$ and $T_0(1)=0$, we obtain the zeroth order solutions

$$u_0=A_1y+A_2, \quad (22)$$

$T_0 = B_1 y + B_2.$ (23)

Solving (17) and (18) and applying the boundary conditions $u_1(0) = 0$ and $u_1(1) = 0$, $T_1(0) = 0$ and $T_1(1) = 0$, we obtain the solutions

$$u_1 = \frac{y^2}{2}\frac{dP}{dx} - Gre\left(\frac{y^2}{2} - \frac{y^3}{6}\right) + \lambda\frac{y^2}{2} + A_3 y + A_4. \quad (24)$$

$$T_1 = \frac{\varepsilon y^2}{2}\frac{dP}{dx} - \frac{Ec\,\mathrm{Pr}\,y^2}{2} + \varepsilon Ec\,\mathrm{Pr}\left(\frac{y^2}{2} - \frac{y^3}{6}\right) + S\left(\frac{y^2}{2} - \frac{y^3}{6}\right)$$
$$- \varepsilon S\left(\frac{y^2}{2} - \frac{y^3}{6} + \frac{y^4}{12}\right) + B_3 y + B_4, \quad (25)$$

Solving (19) and (20) and applying the boundary conditions $u_2(0) = 0$ and $u_2(1) = 0$, $T_2(0) = 0$ and $T_2(1) = 0$, we obtain the solutions

$$u_2 = -\frac{\varepsilon Grey^4}{24} - \varepsilon Ec\,\mathrm{Pr}\,Gre\left(\frac{y^4}{24} - \frac{y^5}{120}\right) - GreS\left(\frac{y^4}{24} - \frac{y^5}{120}\right) + \frac{\varepsilon Grey^3}{12} - \frac{Ec\,\mathrm{Pr}\,Grey^4}{24}$$
$$- \frac{\varepsilon GreSy^3}{24} + \frac{GreSy^3}{18} + \varepsilon GreS\left(\frac{y^4}{24} - \frac{y^5}{60} + \frac{y^6}{360}\right) - \frac{Ec\,\mathrm{Pr}\,Grey^3}{12} + \frac{\varepsilon Ec\,\mathrm{Pr}\,Grey^3}{18}$$
$$- \frac{\lambda\varepsilon y^3}{6} + \frac{\lambda Ec\,\mathrm{Pr}\,y^3}{6} + \frac{\lambda\varepsilon y^2}{4} - \lambda S\left(\frac{y^3}{6} - \frac{y^4}{24}\right) + \frac{\lambda\varepsilon Ec\,\mathrm{Pr}\,y^2}{6} + \frac{\lambda Sy^2}{6} - \frac{\lambda\varepsilon Sy^2}{8} \quad (26)$$
$$- \frac{\lambda y^3}{3}\frac{dP}{dx} - \frac{\lambda^2 y^3}{3} - \frac{\lambda Grey^2}{6} + \frac{3\lambda^2 y^2}{4} + \frac{3\lambda y^2}{4}\frac{dP}{dx} - \lambda Gre\left(\frac{y^2}{2} - \frac{y^3}{6}\right)$$
$$- \lambda\varepsilon Ec\,\mathrm{Pr}\left(\frac{y^3}{6} - \frac{y^4}{24}\right) - \frac{\lambda Ec\,\mathrm{Pr}\,y^2}{4} + \lambda Gre\left(\frac{y^3}{6} - \frac{y^4}{24}\right) + \lambda Gre\left(\frac{y^3}{6} - \frac{y^4}{12}\right)$$
$$+ \lambda\varepsilon S\left(\frac{y^3}{6} - \frac{y^4}{12} + \frac{y^5}{60}\right) + A_5 y + A_6,$$

$$T_2 = \frac{\varepsilon^2 y^2}{2} - \frac{\varepsilon Ec\,\mathrm{Pr}\,y^2}{2} + \varepsilon^2 Ec\,\mathrm{Pr}\left(\frac{y^2}{2} - \frac{y^3}{6}\right) + \varepsilon S\left(\frac{y^2}{2} - \frac{y^3}{6}\right) - \varepsilon^2 S\left(\frac{y^2}{2} - \frac{y^3}{3} + \frac{y^4}{12}\right)$$
$$+ 2\varepsilon^2 S\left(\frac{y^3}{6} - \frac{y^4}{12} + \frac{y^5}{60}\right) - \frac{\varepsilon^2 y^3}{6} + \frac{\varepsilon Ec\,\mathrm{Pr}\,Gry^3}{6} - \varepsilon^2 Ec\,\mathrm{Pr}\left(\frac{y^3}{6} - \frac{y^4}{12}\right) - \frac{\varepsilon^2 Sy^2}{4}$$
$$- \varepsilon S\left(\frac{y^3}{6} - \frac{y^4}{12}\right) + \varepsilon^2 S\left(\frac{y^3}{6} - \frac{y^4}{6} + \frac{y^5}{20}\right) - 2\varepsilon^2 Ec\,\mathrm{Pr}\left(\frac{y^3}{6} - \frac{y^4}{24}\right) - 2\varepsilon S\left(\frac{y^3}{6} - \frac{y^4}{24}\right)$$
$$- \frac{\varepsilon Ec\,\mathrm{Pr}\,y^2}{2} + \frac{\varepsilon^2 Ec\,\mathrm{Pr}\,y^2}{3} + \frac{\varepsilon Sy^2}{3} + \frac{Ec\,\mathrm{Pr}\,y^3}{3}\frac{dP}{dx} + \frac{\lambda Ec\,\mathrm{Pr}\,y^3}{3} - \frac{\lambda Ec\,\mathrm{Pr}\,y^2}{2} \quad (27)$$
$$+ \frac{Ec\,\mathrm{Pr}\,Grey^2}{3} - \frac{Ec\,\mathrm{Pr}\,y^2}{2}\frac{dP}{dx} - \frac{\varepsilon^2 y^3}{3} + \frac{\varepsilon Ec\,\mathrm{Pr}\,Grey^3}{9} - \frac{\varepsilon Ec\,\mathrm{Pr}\,y^3}{3}\frac{dP}{dx}$$
$$+ \frac{\varepsilon^2 y^2}{2} + B_5 y + B_6,$$

Equations (22) - (27) gives the approximation solutions for velocity and temperature as

$$u = u_{.0} + u_1 + u_2 + ... \quad (28)$$

$$T = T_0 + T_1 + T_2 + ..., \quad (29)$$

Where,

$$A_1 = B_1 = -1,\ A_2 = B_2 = 1,$$
$$A_3 = \frac{Ec\,\mathrm{Pr}}{2} - \frac{\varepsilon}{2} - \frac{\varepsilon Ec\,\mathrm{Pr}}{3} - \frac{S}{3} + \frac{\varepsilon S}{4}, \quad B_3 = \frac{Gre}{3} - \frac{\lambda}{2} - \frac{dP}{2dx},$$
$$A_4 = B_4 = A_6 = B_6 = 0,$$
$$A_5 = \frac{\varepsilon Ec\,\mathrm{Pr}}{2} - \frac{\varepsilon^2}{2} - \frac{\varepsilon^2 Ec\,\mathrm{Pr}}{3} - \frac{7\varepsilon S}{24} + \frac{\varepsilon^2 S}{5} + \frac{Ec\,\mathrm{Pr}}{6}\frac{dP}{dx} - \frac{Ec\,\mathrm{Pr}\,Gre}{12} + \frac{\lambda Ec\,\mathrm{Pr}}{6}$$
$$+ \frac{4\varepsilon Ec\,\mathrm{Pr}\,Gre}{45} - \frac{\varepsilon Ec\,\mathrm{Pr}}{6}\frac{dP}{dx} - \frac{\lambda\varepsilon Ec\,\mathrm{Pr}}{6} - \frac{\varepsilon Ec^2\,\mathrm{Pr}^2}{24} + \frac{\varepsilon^2 Ec\,\mathrm{Pr}}{24} - \frac{Ec\,\mathrm{Pr}\,S}{24}$$

$$+\frac{\varepsilon Ec\,\mathrm{Pr}\,S}{45}-\frac{\varepsilon^2 Ec\,\mathrm{Pr}\,S}{24}+\frac{\varepsilon^2 Ec^2\,\mathrm{Pr}^2}{45}+\frac{13\varepsilon Ec\,\mathrm{Pr}\,S}{180}+\frac{S^2}{45}-\frac{\varepsilon S^2}{24}+\frac{\varepsilon^2 S^2}{52},$$

$$B_5=\frac{Ec\,\mathrm{Pr}\,Gre}{24}-\frac{\varepsilon Gre}{24}-\frac{\varepsilon Ec\,\mathrm{Pr}\,Gre}{45}-\frac{GreS}{45}+\frac{\varepsilon GreS}{72}+\frac{7\lambda Gre}{24}-\frac{5\lambda}{12}\frac{dP}{dx}$$

$$-\frac{5\lambda^2}{12}+\frac{\lambda Ec\,\mathrm{Pr}}{12}-\frac{\lambda\varepsilon}{12}-\frac{\lambda\varepsilon Ec\,\mathrm{Pr}}{24}-\frac{\lambda S}{24}+\frac{\lambda\varepsilon S}{40},$$

2.2 Pressure Gradient

In order to find pressure gradient in the present problem, we assumed that the flow has a constant mass flux q and use the assumption to determine the pressure gradient that drives the flow

$$\int_0^1 u(y)dy=q, \tag{30}$$

Where q is the mass flux constant. Then the pressure gradient can be expressed as

$$\frac{dP}{dx}=\frac{A_7}{A_8}, \tag{31}$$

where,

$$A_7=-\frac{1}{2}+\frac{Gre}{24}-\frac{\varepsilon Gre}{120}+\frac{Ec\,\mathrm{Pr}\,Gre}{120}-\frac{\varepsilon Ec\,\mathrm{Pr}\,Gre}{240}-\frac{GreS}{240}+\frac{5\varepsilon GreS}{2016}+\frac{\lambda\varepsilon Ec\,\mathrm{Pr}}{720}+\frac{\lambda S}{720}$$

$$-\frac{\lambda\varepsilon S}{720}+\frac{17\lambda\varepsilon Gre}{720}-\frac{\lambda^{\varepsilon S}2}{24},\quad A_8=\frac{1}{12}+\frac{\lambda}{24}.$$

To find the critical values of Gre after which a reverse flow sets in near the stationary plate, we evaluate $\left.\frac{du}{dy}\right|_{y=1}=0$, and found that

$$Gre_c=\frac{A_9}{A_{10}+A_{11}} \tag{32}$$

where,

$$A_9=-6-\frac{5\lambda}{4}-\frac{\lambda\varepsilon Ec\,\mathrm{Pr}}{30}+\frac{\lambda S}{30}-\frac{\lambda\varepsilon S}{90}-\frac{\lambda^2}{3}-\frac{6}{\lambda}+\frac{Ec\,\mathrm{Pr}}{60}+\frac{S}{60}-\frac{\varepsilon S}{60}-\frac{\lambda\varepsilon}{12}+\frac{31\lambda Ec\,\mathrm{Pr}}{36}-\frac{\lambda S}{24}+\frac{\lambda\varepsilon S}{40}$$

$$+\frac{\lambda^2\varepsilon Ec\,\mathrm{Pr}}{720}+\frac{\lambda^2 S}{720}-\frac{\lambda^2\varepsilon S}{720}-\frac{\lambda^3}{24},$$

$$A_{10}=-\frac{179}{360}+\frac{\varepsilon}{40}-\frac{Ec\,\mathrm{Pr}}{40}+\frac{\varepsilon Ec\,\mathrm{Pr}}{72}+\frac{11S}{360}-\frac{11\varepsilon S}{1260}-\frac{67\lambda}{120}-\frac{1}{2\lambda}+\frac{\varepsilon}{10\lambda}-\frac{Ec\,\mathrm{Pr}}{10\lambda},$$

$$A_{11}=\frac{\varepsilon Ec\,\mathrm{Pr}}{20\lambda}+\frac{S}{20\lambda}-\frac{5\varepsilon S}{168\lambda}+\frac{\lambda\varepsilon}{120}-\frac{\lambda Ec\,\mathrm{Pr}}{12}+\frac{\lambda\varepsilon Ec\,\mathrm{Pr}}{240}+\frac{\lambda S}{240}-\frac{5\lambda\varepsilon S}{2016}-\frac{17\lambda^2}{720}.$$

To obtain the skin friction and rate of heat transfer at both plates, the expression for temperature and velocity are differentiated with respect to y, that is

$$\tau_0=(1-\lambda T)\left.\frac{du}{dy}\right|_{y=0}, \tag{33}$$

$$\tau_1=(1-\lambda T)\left.\frac{du}{dy}\right|_{y=1}, \tag{34}$$

$$Nu_0=(1-\varepsilon T)\left.\frac{dT}{dy}\right|_{y=0}, \tag{35}$$

$$Nu_1=(1-\varepsilon T)\left.\frac{dT}{dy}\right|_{y=1} \tag{36}$$

We further obtain the mass flux Q by evaluating the integral

$$Q=\int_0^1 u dy, \tag{37}$$

Also mean temperature θ_m, we have

$$\theta_m=\frac{\int_0^1 uTdy}{\int_0^1 udy}. \tag{38}$$

3 Results and Discussion

The present problem considers effects of variability in viscosity and thermal conductivity on steady mixed convection flow and heat transfer in a vertical channel using Homotopy Perturbation method controlled by a number of physical parameters such as the variable viscosity (λ), variable thermal conductivity (ε), Prandtl number (Pr), viscous dissipation (Ec), mixed convection parameter (Gre), and heat generation/absorption parameter (S), the constant mass flux (q) and also the critical values of (Gre), which signal the onset of reverse flow near the stationary plate, the skin friction (τ), rate of heat transfer (Nu), pressure gradient $\left(\frac{dP}{dx}\right)$ and mean temperature (θ_m) are presented in tables. In this discussion, the value of Pr used is 0.71 which corresponds to air, the values of S are chosen between -2.0 to 2.0 to account for heat generation $(S<0)$ as well as heat absorption $(S>0)$ through the plates. All other parameters of interest are selected arbitrarily between $0.1 \le Ec \le 1.0$, $5.0 \le Gre \le 25.0, 0$ since the viscosity of air and its thermal conductivity increases with growing temperature, we will consider the viscosity parameter $(\lambda<0)$ and conductivity parameter $(\varepsilon<0)$ throughout this discussion.

Figures 2 and 3 illustrate the effect of Prandtl number on fluid velocity and temperature. Increase in Prandtl number Pr has generated two opposing trends in velocity and temperature within the channels. Near the heated plate, it is observed that fluid velocity increases with an increase in Prandtl number. However, increase in Prandtl number has an increasing effect on velocity near the cold plate as shown in figure 2. On the other hand, the reverse trend is observed in fluid temperature as shown in figure 3. This is physically expected because an increase in Prandtl number Pr decreases the thermal diffusivity of the working fluid, which reduces the thermal boundary layer thickness and energy mobility. Therefore the transmission of heat generated by viscous dissipation reduces as Prandtl number increasing, causing heat accumulation.

The effect of viscous dissipation Ec on the velocity and temperature profiles are observed in figures 4 and 5. It is observed that fluid velocity increases at fluid section adjacent to the heated plate while it decreases at section adjacent to the cold plate as the viscous dissipation increases. However, the reverse trend is observed in fluid temperature as shown in figure 5. Also greater viscous dissipative heat causes rise in velocity as well as temperature and as consequences greater buoyancy force so that fluid velocity increases as viscous dissipation increases.

The effect of mixed convection parameter Gre on the velocity and temperature profiles are presented in figures 6 and 7. Increase in mixed convection parameter has generated two opposing trends in velocity within the channel. Near the heated plate, it is discovered that mixed convection parameter leads to corresponding rise in velocity and the opposite trend is discovered near the cold plate as shown in figure 6. On the other hand, growing mixed convection parameter increased the convection current within the channel so that fluid temperature is observed to increase as mixed convection parameter is increased as shown in figure 7. This is physically true since higher value of mixed convection parameter Gre implies an improved buoyancy force which is higher when compared to the viscous force.

The influence of heat generation/absorption on the fluid velocity and temperature are presented in figures 8 and 9. It should be noted that $(S<0)$ represents heat generation while $(S>0)$ represents heat absorption. It is clearly discovered from the figure 8 that fluid velocity increases near the heated plate as a result of increase of heat generation parameter, while the reverse trend is observed on the cold plate. Moreover, fluid temperature increases as the heat generation $(S<0)$ increases, while it decreases with the increase in heat absorption $(S>0)$. The influence of temperature increase is the strengthening of the convection current which has the capacity to increase the fluid velocity. However, the pressure gradient application is one that maintains a constant flow rate so that velocity is conditioned to decrease near the cold plate.

The influence of viscosity variation λ on the fluid velocity and temperature are shown in figures 10 and 11. It is clearly seen that fluid velocity and temperature increase at fluid section near the heated plate while they decrease at section near the cold plate as the viscosity increases. This is attributed to reduction in diffusivity due to increase viscosity and dominance of applied boundary heating over the viscous dissipation near the heated plate whereas near the cold plate. In addition to these, an increasing viscosity corresponds to the increasing resistance to flow which suppress the velocity of the working fluid, decreasing the viscosity contributes a decrease in the temperature of the working fluid.

The effect of variable thermal conductivity parameter ε on the velocity and temperature profiles are observed in figure 12 and 13. The thermal conductivity ε of the fluid increases the fluid velocity adjacent to the heated plate and decreases adjacent to the cold plate while the reverse case is observed on the fluid temperature. An increase in the thermal conductivity of the fluid which causes an increase in the thermal boundary layer thickness resulting in temperature increase in the channel. The thermal boundary layer thickness is also increased due to the corresponding strengthening of the convection currents caused by increase in the thermal conductivity and fluid velocity increases.

Table 1 exhibits the numerical value of Gre which signaling the onset of reverse flow near the stationary plate. A general view of this table indicates that an increase in the thermal conductivity and heat generation decreases the critical value of Gre for which reverse flow sets in adjacent the plate $(y=1)$. However, mixed convection parameter decreases with the increase in both thermal conductivity and viscosity. In addition to these, an increase in mixed convection parameter increases the reverse flow region and the critical value of the mixed convection parameter leading to the flow reversal. The table further shows that mixed convection parameter increases due to growing heat absorption. That is, it requires a reduced Gre to bring about a reverse flow near the plate whenever the buoyancy is enhanced. On the other hand, the critical value decreases when the working fluid is air as compared to that of mercury.

The skin friction on both boundary surfaces are simulated and presented in table 2. It clearly seen from table 2 that an increase in thermal conductivity have tendency to increase the skin friction on both plates. Furthermore, skin friction decreases as viscosity increases. The table further shows that the skin friction drops when the working fluid is air as compared to that of mercury. This is physically expected since an increase in Prandtl number Pr decreases the thermal diffusivity of the working fluid.

Table 3 presents the numerical values of rate of heat transfer on both boundary surfaces. It is clearly discovered that the rate of heat transfer increases with an increase in thermal conductivity at the heated plate and decreases at the cold plate. This is physically true since fluid temperature increases with an increase in thermal conductivity near the heated plate and decreases near the cold plate. More so, the rate of heat transfer is higher when the working fluid is air as compared to that of mercury. Finally, rate of heat transfer decreases as viscosity increases near the heated plate, the reverse trend is observed near the cold plate.

Table 4 shows the numerical values of mass flux Q. It is discovered that mass flux decreases with an increase in the thermal conductivity. However, mass flux increases with an increase in Prandtl number.

The numerical values of pressure gradient $\left(\frac{dP}{dx}\right)$ and mean temperature (θ_m) are indicated in table 5. An observation from table 5 is that pressure gradient and mean temperature decrease when the thermal conductivity increases. However, pressure gradient increases as viscosity increases while the reverse trend is observed in mean temperature. The table further shows that the pressure gradient increases with an increase in Prandtl number $\Pr$. An increase in Prandtl number requires an increase in pressure gradient.

4 Validation of Results

By setting the mixed convection term Gre, viscous dissipation term Ec, variable viscosity term λ, variable thermal conductivity term ε and pressure gradient $\frac{dP}{dx}$ to zero in the present problem, we recover the results of Jha and Ajibade (2010). The comparison is presented in table 6 which shows that the Homotopy perturbation method is an efficient tool for solving coupled and nonlinear system of differential equations.

5 Conclusions

In this paper the effects of variability in viscosity and thermal conductivity on steady mixed convection flow and heat transfer in a vertical channel. Equations of momentum and energy are obtained and solved using Homotopy perturbation method. The following major findings have been drawn from the present work. The thermal conductivity of the fluid increases the fluid velocity adjacent to the heated plate and decreases adjacent to the cold plate while the reverse case is observed on the fluid temperature. Fluid velocity and temperature increases at fluid section near the heated plate while it decreases at section near the cold plate as the viscosity increases. It was further discovered that a higher mixed convection parameter leads to induce a reverse flow. In addition, a comparison made between present work with those of Jha and Ajibade (2010) shows that the present work agrees significantly with Jha and Ajibade (2010). Finally, thermal conductivity and variable viscosity are important fluid properties.

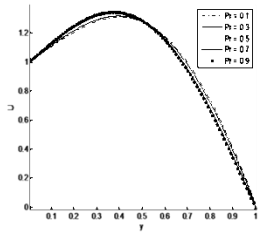

Fig 2: Velocity profile for different values of $\Pr(Ec = 1.0, S = 2.0, \lambda = -0.8, \varepsilon = -0.3, Gre = 15.0, q = 1.0)$

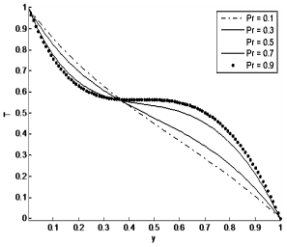

Fig 3: Temperature profile for different values $\Pr(Ec = 1.0, S = 2.0, \lambda = -0.8, \varepsilon = -0.3, Gre = 15.0, q = 1.0)$

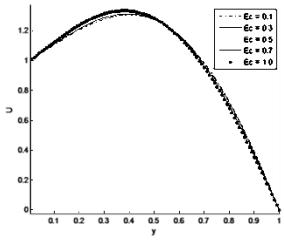

Fig 4: Velocity profile for different values of $Ec(\Pr = 0.71, S = 2.0, \lambda = -0.8, \varepsilon = -0.3, Gre = 15.0, q = 1.0)$

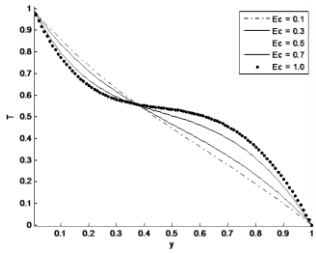

Fig 5: Temperature profile for different values $Ec(\Pr = 1.0, S = 2.0, \lambda = -0.8, \varepsilon = -0.3, Gre = 15.0, q = 1.0)$

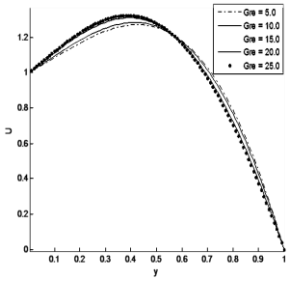

Fig 6: Velocity profile for different values of $Gre(\Pr = 0.71, Ec = 1.0, S = 2.0, \lambda = -0.8, \varepsilon = -0.3, q = 1.0)$

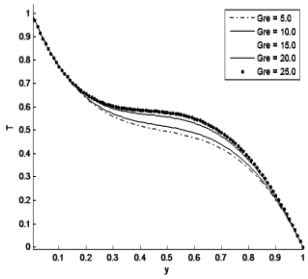

Fig 7: Temperature profile for different values $Gre(\Pr = 0.71, Ec = 1.0, S = 2.0, \lambda = -0.8, \varepsilon = -0.3, q = 1.0)$

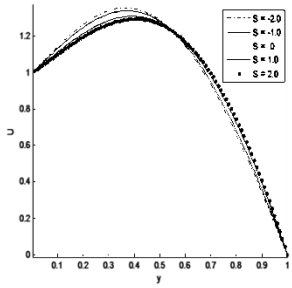

Fig 8: Velocity profile for different values of $S(\Pr = 0.71, Ec = 1.0, \lambda = -0.8, \varepsilon = -0.3, Gre = 15.0, q = 1.0)$

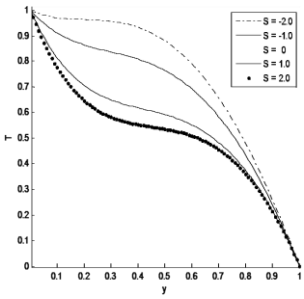

Fig 9: Temperature profile for different values $S(\Pr = 0.71, Ec = 1.0, \lambda = -0.8, \varepsilon = -0.3, Gre = 15.0, q = 1.0)$

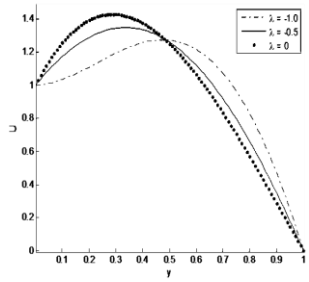

Fig 10: Velocity profile for different values of $\lambda(\Pr = 0.71, Ec = 1.0, S = 2.0, \varepsilon = -0.3, Gre = 15.0, q = 1.0)$

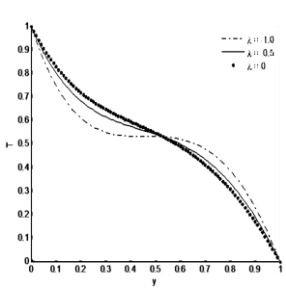

Fig 11: Temperature profile for different values $\lambda(\text{Pr}=0.71, Ec=1.0, S=2.0, \varepsilon=-0.3, Gre=15.0, q=1.0)$

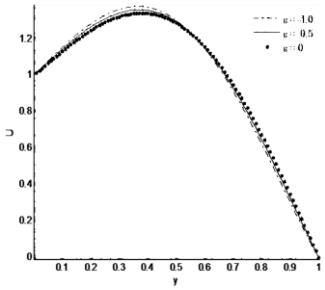

Fig 12: Velocity profile for different values of $\varepsilon(\text{Pr}=0.71, Ec=1.0, S=2.0, \lambda=-0.8, Gre=15.0, q=1.0)$

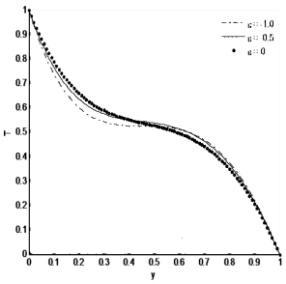

Fig 13: Temperature profile for different values $\varepsilon(\text{Pr}=0.71, Ec=1.0, S=2.0, \lambda=-0.8, Gre=15.0, q=1.0)$

Table 1: Critical values of Gre at the plate $y=1$

		$\lambda=-0.1, \varepsilon=-0.2,$ $Ec=0.6$	$\lambda=-0.1, \varepsilon=-0.5,$ $Ec=0.6$	$\lambda=-0.3, \varepsilon=-0.5,$ $Ec=0.6$
	S	Gre_{c1}	Gre_{c2}	Gre_{c3}
	-2.0	102.20922	102.18867	69.55230
$\text{Pr}=0.044$	-1.0	102.28516	102.26700	74.77785
	1.0	102.46948	102.45901	87.88285
	2.0	102.58285	102.57842	96.25312
	-2.0	102.19963	102.17677	73.54232
$\text{Pr}=0.71$	-1.0	102.27438	102.25354	79.44131
	1.0	102.45553	102.44132	94.48243
	2.0	102.56673	102.55781	102.04279

Table 2: Estimated Numerical Values of Skin Friction τ_0 and τ_1

		$Ec=0.6, Gre=8.0,$ $\lambda=-0.3, S=1.0$		$Ec=0.6, Gre=8.0,$ $\lambda=-0.3, S=1.0$	
	ε	τ_0	τ_1	τ_0	τ_1
	-1.0	2.75589	3.73610	2.71891	3.45770
$\text{Pr}=0.044$	-0.5	2.78275	3.76150	2.74885	3.47819
	0.5	2.83647	3.81231	2.80872	3.51912
	1.0	2.86334	3.83771	2.83866	3.53959
	-1.0	2.72576	3.67736	2.68324	3.40954
$\text{Pr}=0.71$	-0.5	2.75610	3.71441	2.71761	3.43963
	0.5	2.81678	3.78850	2.78636	3.49982
	1.0	2.84712	3.82554	2.82073	3.52991

Table 3: Estimated Numerical Values of Rate of Heat Transfer Nu_0 and Nu_1

		$Ec=0.6, Gre=8.0,$ $\lambda=-0.3, S=1.0$		$Ec=0.6, Gre=8.0,$ $\lambda=-0.3, S=1.0$	
	ε	Nu_0	Nu_1	Nu_0	Nu_1
	−1.0	1.07569	1.24554	1.06871	1.25261
Pr = 0.044	−0.5	1.13208	1.08211	1.12663	1.08640
	0.5	1.67686	0.62821	1.67489	0.62692
	1.0	2.16523	0.33773	2.16523	0.33365
	−1.0	1.97983	2.16009	1.87585	2.27850
Pr = 0.71	−0.5	1.71466	1.73586	1.63196	1.80853
	0.5	1.72310	0.57127	1.69240	0.55248
	1.0	1.99670	0.16908	1.99670	0.23361

Table 4: Estimated Numerical Values of Mass Flux Q

		$Ec=0.6, Gre=8.0,$ $\lambda=-0.3, S=1.0$	$Ec=0.6, Gre=8.0,$ $\lambda=-0.3, S=1.0$
	ε	Q	Q
	−1.0	0.77748	0.79853
Pr = 0.044	−0.5	0.75383	0.77474
	0.5	0.70653	0.72717
	1.0	0.68288	0.70339
	−1.0	0.81261	0.83688
Pr = 0.71	−0.5	0.78222	0.80640
	0.5	0.72143	0.74546
	1.0	0.69104	0.71498

Table 5: Estimated Numerical Values of Pressure Gradient $\frac{dP}{dx}$ and θ_m

		$Ec=0.6, Gre=8.0,$ $\lambda=-0.3, S=1.0$		$Ec=0.6, Gre=8.0,$ $\lambda=-0.3, S=1.0$	
	ε	$\frac{dP}{dx}$	θ_m	$\frac{dP}{dx}$	θ_m
	−1.0	−60.17032	0.90606	−85.79576	0.87124
Pr = 0.044	−0.5	−55.53653	0.67236	−83.19408	0.64371
	0.5	−46.80655	0.15803	−73.65516	0.14400
	1.0	−42.68983	0.12585	−68.70960	0.13121
	−1.0	−70.71773	0.99907	−95.51063	0.95847
Pr = 0.71	−0.5	−64.21982	0.73535	−89.91547	0.70217
	0.5	−52.14159	0.14125	−78.16144	0.12671
	1.0	−46.52556	0.19500	−71.98320	0.19781

Table 6: Comparison of Numerical Values between the Present Problem and Jha and Ajibade (2010)

	Jha and Ajibade (2010) $Gre = 10.0, q = 1.0)$		Present Work $Gre = 10, \Pr = 0.71, Ec = \lambda = \varepsilon = 0, y = 0.5$	
S	Temperature	Velocity	Temperature	Velocity
-1.0	0.56975	1.19747	0.56901	1.19813
-0.5	0.53297	1.19747	0.53289	1.16156
-0.5	0.47030	1.19747	0.47039	1.09412
1.0	0.44341	1.19747	0.44401	1.06609

References

[1] Jha, B. K. (1991). Unsteady mixed convection flow past an infinite vertical porous plate with constant heat source. *Astrophysics and Space Science. 175: 101-105.*

[2] Jha, B. K., and Ajibade, A. O. (2010). Unsteady free convective Couette flow of heat generating/absorbing fluid. *International Journal of Energy and Technology. 2(12), (2010): 1-9.*

[3] Jer-Huan, J., Han-Chieh, C., and Wei-Mon, Y. (2010). Wall transpiration effects on developing mixed convection heat transfer in inclined rectangular ducts. *Journal of Marine Science and Technology. 18(2):249-258.*

[4] Jha, B. K., Debora, D., and Ajibade, A. O. (2013). Steady fully developed mixed convection flow in a vertical parallel micro-channel with bilateral heating and filled with porous material. *Journal of Process Mechanical Engineering. 227(1): 56-66.*

[5] Hamid, N., and Behnam, R. (2013). Mixed convective rarefied flows with symmetric and symmetric heated walls. *Computational thermal Sciences. 5(4): 261-272.*

[6] Borah, G., and Hazarika, G. C. (2013). Effects of variable viscosity and thermal conductivity and magnetic field effect on the free convection and mass transfer flow through porous medium with constant suction/heat flux. *Journal of Comp and Math. Scie. 4(6): 407-418.*

[7] Hazeem, A. A., and Mostafa A. M. A. (2013). On the effectiveness of variation of physical variables on steady flow between parallel plates with heat transfer in a porous medium. *Journal of Theoretical and Applied Mechanics. 51(1): 53-61.*

[8] Mohamed, A. (2014). Unsteady mixed convection heat transfer along vertical stretching surface with variable viscosity and viscous dissipation. *Journal of Egyptian Mathematical Society. 22: 529-537.*

[9] Swati, M., and Iswar, C. M. (2015). Magnetohydrodynamics mixed convection slip flow and heat over a vertical porous plate. *Engineering Science and Technology an International Journal. 18: 98-105.*

[10] Parash, M. T., and Hazarika, G. C. (2015). Effects of variable viscosity and thermal conductivity on unsteady free convective heat and mass transfer MHD flow of micropolar fluid with constant heat flux through a porous medium. *International Journal of Computer Applications. 110(8): 0975-8887.*

[11] Anjali-Devi, S. P., and Prakash, M. (2015). Temperature dependent viscosity and thermal conductivity effects on hydromagnetic flow over a slendering stretching sheet. *Journal of Nigerian mathematical Society.34: 318-330.*

[12] Makungu, J., Mureithi, E. W, and Dinitry, K. (2015). Effect of variable viscosity of Nanofluid over a permeable wedge embedded in saturated porous medium with chemical reaction and thermal radiation. *International Journal of Advances in Applied Mathematics and Mechanics. 2(3): 101-118.*

[13] Santana, H. and Hazarika, G. C. (2015). Effects of variable viscosity and thermal conductivity on MHD free convection and mass transfer flow over an inclined vertical surface in a porous medium with heat generation. *International Journal of Engineering and Science. 4(8): 20-27.*

[14] Macha, M., and Naikoti, K. (2016). Mixed convection analysis of heat and mass transfer. *Journal of Egyptian Mathematical Society. 24:458-470.*

[15] Muhammad, K. A. M., Norhafizah, M. S., Nor, A. Z., Mohammed, Z. S., and Anuar, I. (2016). Viscous dissipation effect on the mixed convection boundary layer flow towards solid sphere. *Transaction on Science and Technology. 3(1-2): 59-67.*

[16] Prathap, J. K., Umavathi, J. C., and Prasad, M. K. (2016). Effect of viscous dissipation on mixed convection flow in a vertical double passage channel using Robin boundary conditions. *International Journal of Engineering, Science and Technology. 8(3):27-47.*

[17] Hazarika, G. C. and Bandita, P. (2016). Effects of variable viscosity and thermal conductivity on MHD free convection flow of a micropolar fluid past a stretching plate through porous medium with radiation, heat generation and joule dissipation. *Turk. J. Phys. 40: 40-51.*

[18] Ajibade, A. O., and Thomas, U. O. (2017). Entropy generation and irreversibility analysis due to steady mixed convective flow in a vertical porous channel. *International Journal of Heat and Technology. 35(3):433-446.*

[19] Jha, B. K., and Aina, B. (2017). Effect of induced magnetic field on magnetohydrodynamics mixed convection flow in a vertical micro-channel. *International Journal of Applied Mechanics and Engineering. 22(3):567-582.*

[20] Ajibade, A. O., and Tafida, M. K. (2019). Viscous dissipation effect on steady natural convection Couette flow of heat generating fluid in a vertical channel. *Journal of advances in Mathematics and Computer Science. 30(1):1-16.*

[21] Ajibade, A. O, and Tafida, M. K. (2019).Viscous dissipation effect on a steady generalized Couette flow of heat generating/absorbing fluid in a vertical channel. *Z. Naturfursch. 74(7)a: 605-616.*

[22] He, J. H. (1999). Homotopy Perturbation Methods Technique, *Computer Method in Applied Mechanics and Engineering. 178, (1999), 257-262.*

[23] He, J. H. (2000). A coupling method of a homotopy technique and a perturbation technique form on non-linear problems. *Int. J. Non-linear Mech. 35: 37-45.*

[24] He, J. H. (2003). Homotopy Perturbation Methods a new non-linear analytical technique. Applied Math. Comput. 135:73-79.
[25] He, J. H. (2004). A coupling method of a homotopy technique and a perturbation technique form on non-linear problems. Appl. Math. Comput. 3: 151-158.
[26] Abaker, A. H. (2017). Analytical solution of linear and non linear Schrodinger equation using Homotopy perturbation method and variational iterative method. American Journal of Engineering Research (AJER). 6(3): 107-114.
[27] Abou-Zeid, M. (2017). Homotopy perturbation method for magnetohydrodynamics non- Newtonian nano fluid flow through a porous medium in eccentric annuli with peristalsis. *Thermal Science. 21: 2058-2069.*